

# Dynamic and static properties of SBS triblock copolymer and their blends

Ging-Ho Hsiue and Mu-Yuan M. Ma

Polymer Research Institute, National Tsing Hua University, Hsinchu, Taiwan, ROC

(Received 18 October 1982; revised 19 July 1983)

By using a dynamic testing method (Rheovibron), it has been established that for a pure triblock copolymer (styrene-butadiene-styrene, SBS), the morphology is composed of a continuous phase, a dispersed phase and an interphase. The predominance of the phase depends upon whether the polymer is cast from a good or poor solvent for each block. For the blends of SBS with PS and PBd, the interphase occupies a greater fraction as indicated by the fact that its corresponding molecular relaxation temperature range is much broader (10°–80°C) than that of pure SBS (60°–80°C). If the blends of SBS with its corresponding homopolymers are heated at 140°C for 45 min, the fraction of the interphase increases significantly and the onset of molecular relaxation is lowered to –10°C. The viscosities of SBS and their blends are measured by both dynamic and static methods. Complex viscosities calculated from the dynamic method show transitions similar to those of storage moduli. Viscosities at different temperatures from these two methods are superimposed onto master curves.

(Keywords: SBS triblock copolymer; dynamic; static; viscosity; blend; deformation)

## INTRODUCTION

To explain the unique physical properties of SBS triblock copolymers, Holden<sup>1</sup> has proposed a molecular arrangement, in which domains of polystyrene (PS) aggregates are dispersed in a matrix of polybutadiene (PBd) continuums due to incompatibility between the PS and PBd blocks. Generally, factors affecting the morphology are considered to be St/Bd weight ratio<sup>2</sup>, casting solvent<sup>2–5</sup>, processing method<sup>6</sup> and thermal history<sup>7,8</sup>. It has been established that the solubility parameter of a solvent has a marked influence on the viscosity of the polymer solution<sup>9</sup>. Solutions of SBS show a maximum viscosity in a solvent having a solubility parameter either slightly higher than that of PS or slightly lower than that of PBd. When the solubility parameter of casting solvent has a value between that of PS and PBd, the viscosity of the polymer solution is much lower and the molecular mobility of each segment is much greater<sup>10</sup>. Therefore, the interdiffusion of both segments into each other are much easier. As a result, the interphase between domains and matrix became much more diffuse and increase in thickness after the evaporation of solvent.

A method called 'solvent sorption analysis' has been used by Chiang *et al.*<sup>11</sup> to investigate the morphology of SBS triblock copolymers. They established that the diffusion rate of solvent vapour through the copolymer film is a function of time and vapour concentration (non-Fickian behaviour), and is different from that of conventional vulcanized rubber (Fickian behaviour). The reason for this abnormal behaviour was attributed to the slow rearrangement of interfacial molecules in attaining equilibrium between the solvent and polymer molecules. Shen *et al.*<sup>12</sup> concluded that at temperatures between –70° and 80°C, the molecular mechanism for stress relaxations were contributed to by an interfacial phase that in-

tervened the PBd continuum and the spherical PS domains. This interphase could be visualized as a series of spherical shells enclosing each of the pure PS domains and characterized by a reasonably sharp concentration gradient between shells of mixed PBd and PS segments.

In this paper, dynamic properties of SBS triblock copolymers and their blends with PS, PBd and SBR are investigated. The results are related to the morphology of these samples cast from solvents with different solubility parameters. It has been shown in the literature<sup>13–15</sup> that the most important factors concerning the blending of triblock copolymer with its corresponding homopolymers are the molecular weights and the fractions of each component. To attain any degree of compatibility, the molecular weights of the added homopolymers cannot exceed the molecular weight of the corresponding block. Otherwise, the homopolymers would not swell into the domains. Moreover, the weight fraction of the triblock copolymer in the system must be >50% to prevent macrophase separation of the system. Accordingly, the molecular weights of the PS block, PBd and the corresponding homopolymers must be determined accurately. Because neither the universal calibration curve nor the standard PS calibration curve can be used in determining the exact molecular weight of triblock copolymers<sup>16</sup>, a technique developed by Runyon *et al.*<sup>17</sup> i.e. 'weighted average method', is used here, as shown in equation (1):

$$\log \bar{M}_c = X_s \log \bar{M}_s + X_b \log \bar{M}_b \quad (1)$$

where  $\bar{M}_c$  is the molecular weight of SBS triblock copolymers at the summit of molecular weight distribution curve;  $\bar{M}_s$  and  $\bar{M}_b$  denote the molecular weights of homo-PS and homo-PBd at the same elution volume as  $\bar{M}_c$ , respectively;  $X_s$  and  $X_b$  are the weight fractions for PS

and PBd block in SBS, respectively. They also discovered that at the same elution volume, the molecular weight of homo-PS was 1.75 times the molecular weight of homo-PBd, thus equation (1) can be converted into equation (2):

$$\log \bar{M}_c = X_s \log \bar{M}_s + (1 - X_s) \frac{\bar{M}_s}{1.75} \quad (2)$$

in which  $\bar{M}_c$  can be easily calculated provided that the weight fraction of PS block and standard PS calibration curve are known. The molecular weights of PS and PB block can also be calculated similarly.

Further, changes of viscosity can be compared at small (dynamic) and large (static) deformation rates. Complex viscosities are obtained through the use of equations (3)–(5).

$$E' = 3G' \quad (3)$$

$$E'' = 3G'' \quad (4)$$

$$\eta^* = (G'^2 + G''^2)^{1/2} / \omega \quad (5)$$

By assuming that the tension is an isotropic one (Poisson ratio = 0.5), the shear modulus can be obtained by dividing  $E'$  and  $E''$  by 3. Here  $E'$  and  $G'$  denote the tensile and shear storage modulus, respectively;  $E''$  and  $G''$  denote the tensile and shear loss modulus, respectively;  $\eta^*$  is the complex viscosity and  $\omega$  is the test frequency. Equations (6)–(8) are used to calculate the shear viscosities from the static method<sup>18</sup>.

$$\alpha = (F/A)\epsilon \quad (6)$$

$$\epsilon = (1/\alpha) (d\alpha/dt) \quad (7)$$

$$\eta(\epsilon') = (\alpha/\epsilon') (1/3) \quad (8)$$

Again the factor 1/3 is used to obtain shear viscosity from elongational viscosity.  $\alpha$  and  $F$  denote the tensile stress and tensile force, both of them are measured at the yield point on a stress–strain plot;  $A$  and  $\epsilon$  denote the cross-sectional area of the sample and the extension ratio at yield point;  $\epsilon'$  and  $\eta(\epsilon')$  denote the strain rate and shear viscosity, respectively.

Finally, an attempt is made to construct and combine together the master curves at these two extremes. The shift factor  $a_T$  is obtained from equation (9). Following the procedure of Arnold *et al.*<sup>19</sup> the density change within the temperature range of the experiment is neglected. The subscript zero in equation (9) represents the properties at the reference state. The reduced time scale is obtained by using equation (10).

$$a_T = T_0 \eta_0 \rho_0 / T \eta_0 \rho \quad (9)$$

$$\omega_{\text{red}} = \omega / a_T \quad (10)$$

## EXPERIMENTAL

### Materials and characterizations

Table 1 gives the characterization data of the polymers used in this experiment. The low molecular weight PS (PS3 and PS6) were synthesized by anionic polymerization in a vacuum line system. The initiator used was a complex of sodium and naphthalene described by Szwarc *et al.*<sup>20</sup> As shown in Table 1, two types of PS were used in this work, one with a molecular weight greater than the PS block in SBS, the other with a molecular weight similar to that of PS block. SBS triblock copolymers and PB homopolymers were obtained from Shell Chemical Co. (Kraton 1101) and Japan Synthetic Rubber Co. (BR01),

respectively. The styrene–butadiene copolymer was a commercial product obtained from Taiwan Synthetic Rubber Co. (Taipol 1502).

### Casting solvents and blending

The characteristics of casting solvents are given in Table 2. They were selected on the consideration of their solubility parameters only. Blending of SBS with the corresponding homopolymers was carried out by solution mixing. A 5% solution of polymer or polymer blends was poured onto the surface of mercury which had been purified with diluted nitric acid beforehand. After the solvent was evaporated for 5 days, the last traces of solvent were eliminated *in vacuo* at room temperature for 24 h. During casting, due to the poor solvation power of EAc towards PB, a solvent mixture of EAc and THF was used to avoid macrophase separation of the polymer film. However, as indicated by the lower boiling point of THF (66°C) than EAc (77°C), the former will evaporate first; therefore, the solvent determining the final physical state of the polymer film is still EAc.

Table 1 Characterization of polymers

Polymer	Molecular weight <sup>a</sup>	Microstructures <sup>b</sup>
Kraton 1101 (SBS)	92 000 $\bar{M}_s = 13\,000$ $\bar{M}_b = 64\,400$	St/Bd = 30/70 <sup>c</sup> vinyl = 8.9%, <i>cis</i> -1.4 = 6.8% <i>trans</i> -1.4 = 44.3%
BR 01	$\bar{M}_w = 311\,000$ $\bar{M}_n = 25\,500$	vinyl = 3.8%, <i>cis</i> -1.4 = 89.5% <i>trans</i> -1.4 = 6.7%
Taipol 1502 (SBR)	$\bar{M}_w = 53\,000$ <sup>c</sup> $\bar{M}_n = 12\,000$	St/Bd = 26.74
PS3	$\bar{M}_w = 49\,000$ $\bar{M}_n = 27\,000$	Atactic
PS6	$\bar{M}_w = 15\,700$ $\bar{M}_n = 9850$	Atactic

<sup>a</sup> Determined by gel permeation chromatography

<sup>b</sup> Determined by infrared spectra and n.m.r. spectra

<sup>c</sup> Obtained from manufacturer

Table 2 Characteristics of casting solvents<sup>a</sup>

Solvent	Solubility parameter <sup>b</sup> (cal cm <sup>-3</sup> ) <sup>1/2</sup>	Descriptions
Cyclohexane (CH)	8.2	Solvent for PBd; solvent for PS at >35°C
Carbon tetrachloride (CCl <sub>4</sub> )	8.6	Good solvent for PBd and PS
Ethyl acetate (EAc)	9.1	Good solvent for PS; poor solvent for PBd
Tetrahydrofuran (THF)	9.1	Solvent for PBd; good solvent for PS

<sup>a</sup> All data from ref. 21

<sup>b</sup> The solubility parameters<sup>21</sup> of PS and PBd are 9.1 and 8.4 (cal cm<sup>-3</sup>)<sup>1/2</sup>, respectively

Dynamic and static experiments

Dynamic mechanical properties were measured by using a Rheovibron Direct-Reading Viscoelastometer, Toyo Baldwin Co., (Model DDV-II-C) operated at a frequency of 3.5 Hz to obtain better resolution of molecular relaxations. The temperature range was  $-90^{\circ}$  to  $110^{\circ}\text{C}$ , and the dimensions of test specimen were  $3\text{ cm} \times 0.5\text{ cm} \times 0.05\text{--}0.06\text{ cm}$ . Static tests were carried out by using an Instron Universal Tensile Tester (Model 1122) with a temperature adjustable chamber. Measurements were taken at 35, 65 and  $80^{\circ}\text{C}$ . The cross-head speeds were 20, 50, 100 and  $200\text{ mm min}^{-1}$ , and the thickness of the test specimen (dumbbell shaped) was between 0.05 and 0.1 cm.

RESULTS AND DISCUSSION

Dynamic properties (small deformation)

Dynamic mechanical spectra of SBS and their blends are shown in Figures 1-6. There is a marked difference between the SBS cast from  $\text{CCl}_4$ , CH, and a mixture of THF and EAc. The most significant differences were the intensities of relaxation peaks and the appearance or disappearance of molecular relaxation between  $60^{\circ}$  and  $80^{\circ}\text{C}$ . For the sample cast from THF/EAc, the morphology of SBS was affected mainly by EAc, which was considered to be a good solvent for PS segments but a poor solvent towards PBD segments. Thus, expansion of PS chains and agglomeration of PBD chains were expected to occur during the formation of polymer film to give a morphology of dispersed PBD phase embedded in continuous PS phase. This resulted in a marked change in the relative intensities of PBD and PS relaxation peaks. As there was a continuous rigid phase (PS), it also exhibited a higher storage modulus than samples obtained from  $\text{CCl}_4$  and CH (Figure 1). However, the lack of molecular

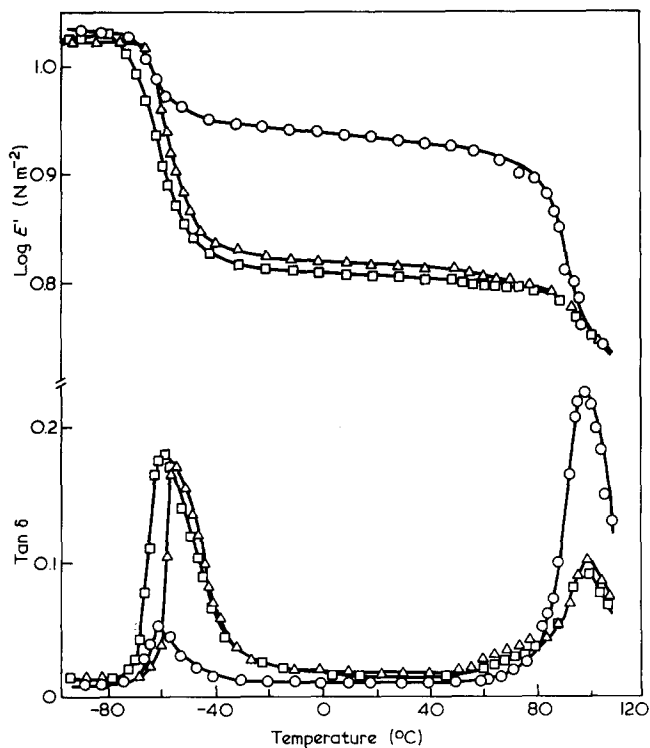


Figure 1 Dynamic loss tangent and storage modulus versus temperature.  $\Delta$ , SBS from  $\text{CCl}_4$ ;  $\square$ , SBS from cyclohexane;  $\circ$ , SBS from THF(50)/EAc(50)

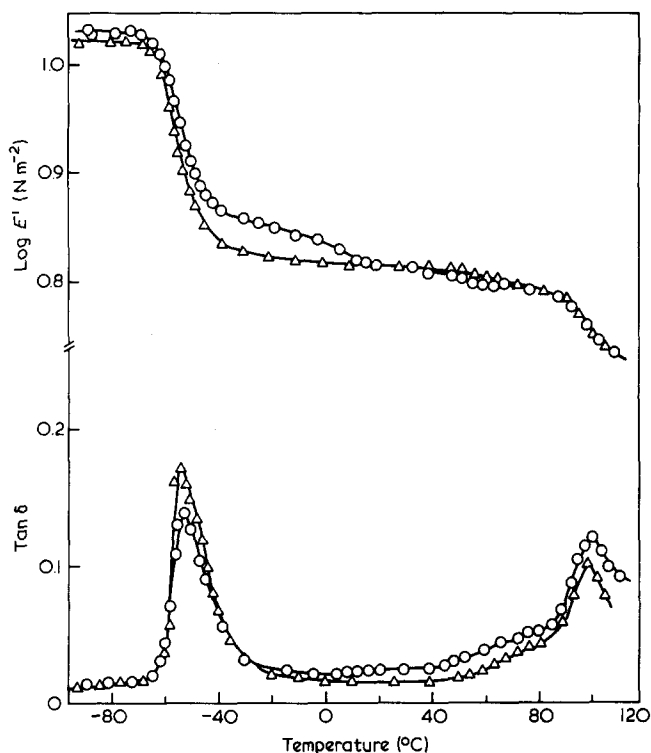
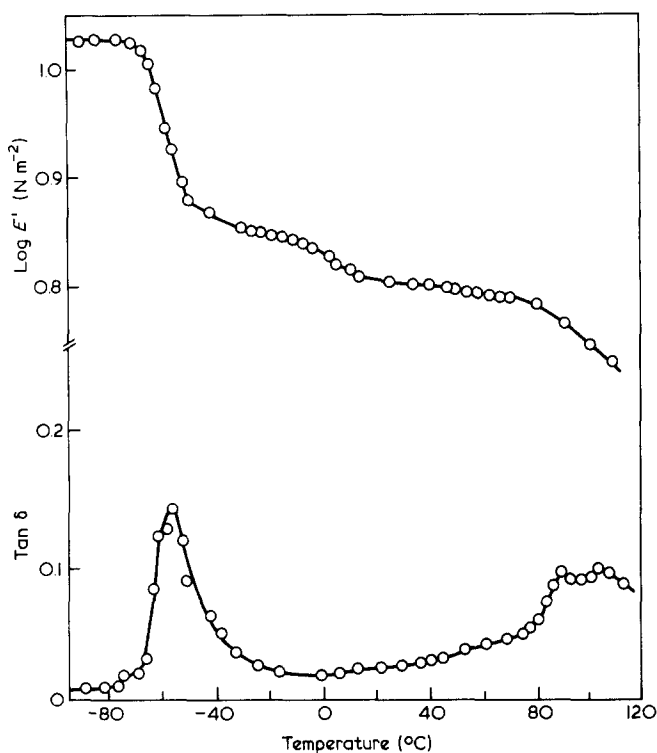


Figure 2 Dynamic loss tangent and storage modulus versus temperature.  $\Delta$ , SBS from  $\text{CCl}_4$ ;  $\circ$ , SBS(70) + PS6(15) + PBD(15) from  $\text{CCl}_4$

relaxation between  $60^{\circ}$  and  $80^{\circ}\text{C}$  is believed to be due to the absence of an interphase between domains and matrix. Because EAc was a good solvent for PS segments only, interdiffusion of polymer chains into one another would be more difficult than in other systems (e.g.  $\text{CCl}_4$  and CH) during the formation of the polymer film. For samples cast from  $\text{CCl}_4$  and CH, the morphologies are believed to be composed of a continuous PBD phase, a dispersed PS phase and an interphase. The appearance of an interphase is attributed to a greater molecular mobility and, hence, greater interdiffusing ability of each segment into one another in mutually good solvents. Thus, the presence or absence of an interphase was entirely dependent upon the properties of the casting solvent. As for the composition of the interphase, the broad molecular relaxations appeared between  $60^{\circ}$  and  $80^{\circ}\text{C}$  indicating that the interphase was a PS-rich phase with a concentration gradient of each segment.

Figure 2 gave the dynamic mechanical spectra of SBS and its blend with PS and PBD homopolymers cast from  $\text{CCl}_4$ . It was established that the fraction of interphase was greatly increased, and the temperature range was broadened from  $10^{\circ}$  to  $80^{\circ}\text{C}$ . These results indicate that appearance of this shoulder on dynamic mechanical spectra was completely due to the presence of interphase, not due to the side-chain relaxations of PS block proposed by Beamish *et al.*<sup>22</sup>. Furthermore, these results resembled those obtained by Shen *et al.*<sup>12</sup> who claimed that the outermost shell of the interphase displayed the lowest concentration of PS segments. Both the transition temperature and the volume fraction of PS segments increased rapidly in succeeding interior shells. As a result, an increase in thickness of the interphase leads, of course, to an increased concentration gradient of either segments as well as a broadening of relaxation temperature range. According to Meier's theory<sup>23</sup>, the fraction of interphase



**Figure 3** Dynamic loss tangent and storage modulus versus temperature.  $\circ$ , SBS(70) + PS3(15) + PBd(15) from  $\text{CCl}_4$

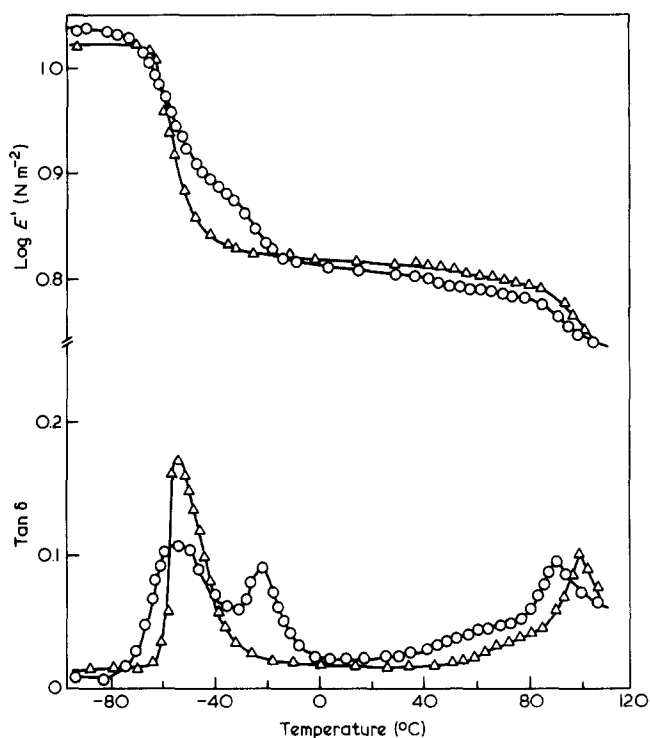


**Figure 4** Dynamic loss tangent and storage modulus versus temperature.  $\Delta$ , SBS from  $\text{CCl}_4$ ;  $\circ$ , SBS(80) + SBR(20) from  $\text{CCl}_4$

in SBS should be much more than that in a purely homopolymer blend. However, here, SBS eventually only acted as a compatibilizer, the added PS would swell completely into the PS domains and consequently the molecular weights of both PS homopolymer and PS block are similar. Therefore, it would loosen the PS domains and enhance the tendency for interfacial mixing of PS and

PBd segments. Figure 3 shows the results when the molecular weight of the added PS (PS3) was much higher than that of the PS block. As expected, it gave two PS transitions which were identical to those obtained by Krause *et al.*<sup>15</sup>. As for the interphase, its behaviour was the same as in the sample blended with PS6. In the blend of SBS with St-Bd random copolymers (Figure 4), the fraction of interphase was greater than that in pure SBS. However, the temperature indicating the onset of molecular relaxations of interphase was 40°C, which was considerably higher than that previously. The reason for this may be attributed to the  $T_g$  of SBR itself (-23°C as shown by the third peak in the dynamic spectrum). In the formation of domains and matrix, the molecules of SBR, which possessed a  $T_g$  much higher than that of the PBd homopolymers used formerly, also participated in the formation of the interphase; therefore, an increase in the onset temperature of molecular relaxations of the interphase should be expected.

Figures 5 and 6 show the dynamic mechanical spectra of samples which were thermally treated. Beamish *et al.*<sup>22</sup> discovered that, upon annealing, the shoulder for the interfacial transition was reduced. But in the data here, this shoulder still remained after the sample was annealed at the transition temperature of the interphase (70°C) for 12 h (Figure 5). The reason for this discrepancy might be due to insufficient temperature and duration for annealing as compared to the conditions used by Beamish *et al.* (153°C for 1 week). However, when the sample was heated at 145°C for 45 min then quenched in liquid nitrogen to retain the morphology of the blends at that temperature, the result (Figure 6) was completely opposite to that obtained by Beamish *et al.* In this case, a volume fraction of the interphase greater than all the other samples was obtained. As shown in the Figure, there was a tendency for the added PS homopolymers to escape from the PS

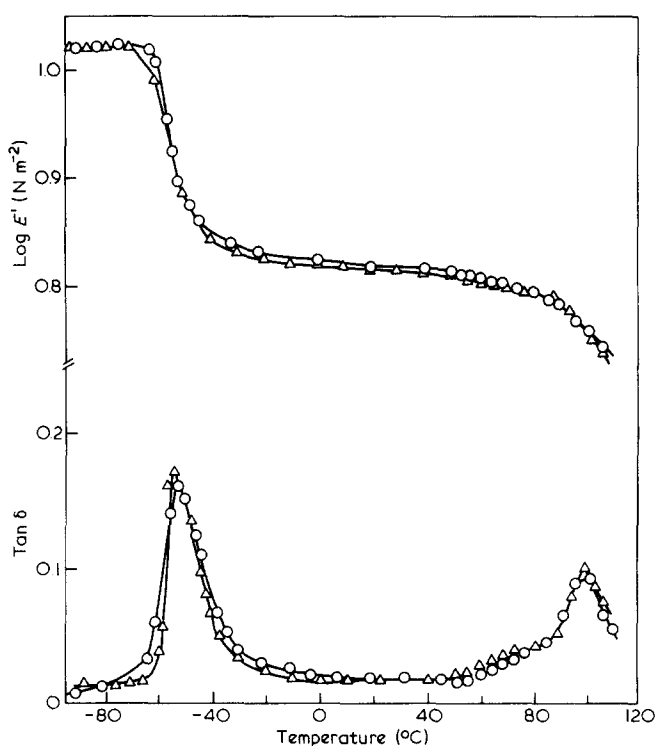


**Figure 5** Dynamic loss tangent and storage modulus versus temperature.  $\Delta$ , SBS from  $\text{CCl}_4$ ;  $\circ$ , SBS from  $\text{CCl}_4$  annealed at 70°C for 12 h

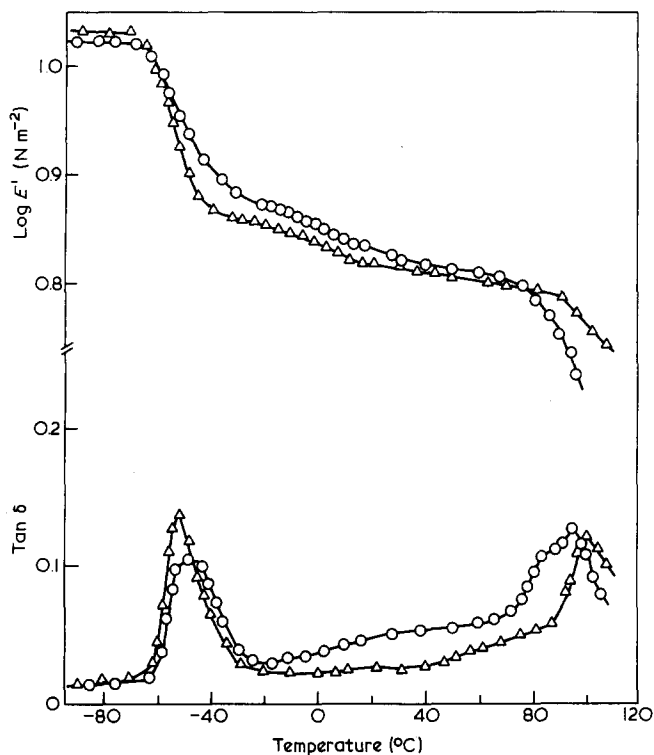


**Figure 6** Dynamic loss tangent and storage modulus versus temperature.  $\Delta$ , SBS(70)+PS6(15)+PBd(15) from  $\text{CCl}_4$ ;  $\circ$ , SBS(70)+PS6(15)+PBd(15) from  $\text{CCl}_4$  heated at  $140^\circ\text{C}$  for 45 min then quenched

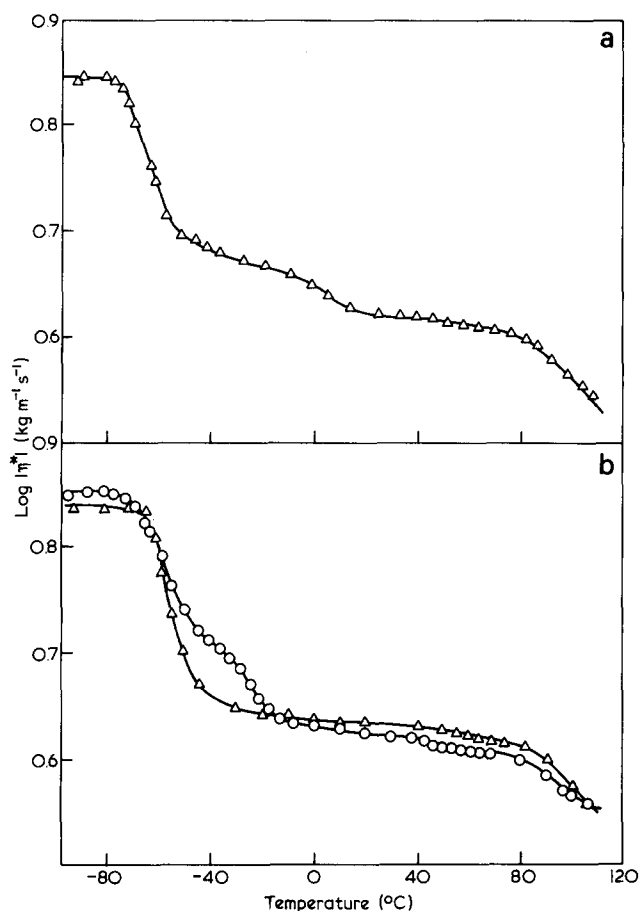


**Figure 8** Complex viscosity versus temperature. (a):  $\Delta$ , SBS(70)+PS3(15)+PBd(15) from  $\text{CCl}_4$ . (b):  $\Delta$ , SBS from  $\text{CCl}_4$ ;  $\circ$ , SBS(80)+SBR(20) from  $\text{CCl}_4$

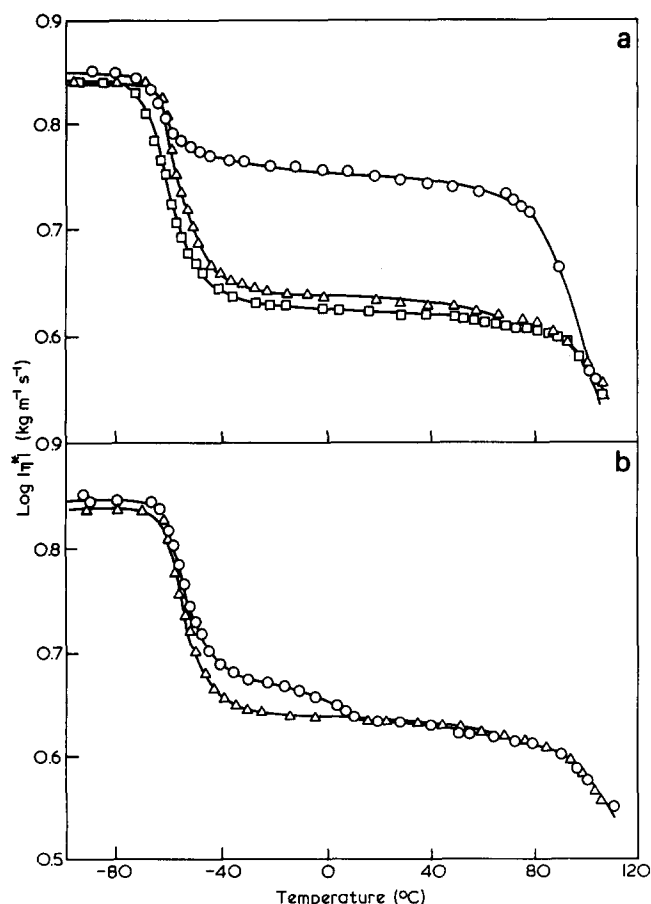


**Figure 7** Complex viscosity versus temperature. (a):  $\Delta$ , SBS from  $\text{CCl}_4$ ;  $\square$ , SBS from cyclohexane;  $\circ$ , SBS from THF(50)/EAc(50). (b):  $\Delta$ , SBS from  $\text{CCl}_4$ ;  $\circ$ , SBS(70)+PS6(15)+PBd from  $\text{CCl}_4$

domains. The broadening of temperature range for molecular relaxations of the interphase from  $-10^\circ$  to  $80^\circ\text{C}$  also indicated that the thickness (volume fraction) of the interphase was being increased.

Figures 7–9 show the complex viscosities calculated from equations (3)–(5) versus temperature. These curves show similar transitions to those for the storage moduli; i.e. two steep and one smooth decrease representing the transitions of PBd, PS and the interphase, respectively. The viscosities are believed to be affected mainly by domain integrity, free volume, volume fraction of rigid phase, and molecular weights. For pure SBS, the dominant factor affecting the viscosities was the volume fraction of the rigid phase. For the samples used, the one cast from THF(50)/EAc(50) had the highest viscosity (Figure 7a) as expected. For samples cast from  $\text{CCl}_4$  and CH, there was only a slight difference which was due to the preferential solvation of solvents toward each block individually. As for the blends (Figures 7b and 9b), factors affecting the behaviour of viscosity were too complicated to be resolved. However, in the dynamic test, the samples were placed in a state of small deformation (less than 1%); therefore, some factors which would create notable differences were not clear.

*Static properties (large deformation)*

By using equations (6)–(8), changes of shear viscosities (Figures 10 and 11) for each sample at three different temperatures were measured using the Instron and calculated from their corresponding stress–strain plots. Among

them, SBS cast from THF/EAc (Figure 10a) had the highest viscosity as in the dynamic test. However, for SBS cast from CH and CCl<sub>4</sub> (Figures 11a and b), the viscosities obtained were considerably lower; this may be due to the influence of less rigid phase contents. The viscosities of SBS cast from CCl<sub>4</sub> were also higher than that cast from CH. The reason for this phenomenon may be attributed to

a larger free volume in the latter case due to the better solvation ability of CH towards PBd segments. As for the blends, the viscosities were, undoubtedly higher than pure SBS due to the influences of the molecular weights of added SBR and PBd (Figures 10b and c). As mentioned previously, domain integrity also are important in determining the viscosity behaviour. The lower viscosities of the ternary system (SBS + PS6 + PBd, Figure 10c) and the higher viscosities of the binary system (SBS + SBR, Figure 10b) is attributed to the influences of the loose domains and the compact domains occurring within them.

*Time-temperature superposition*

The viscosities obtained from small and large deformations were all superimposed into master curves by using equations (9) and (10). In both cases (Figures 12-15) the curves were converted into smoother ones versus reduced frequency. However, when the curves from those two tests were combined, the agreements between them were not so good owing to inherent differences in characteristics of these two methods. Again, for the samples of pure SBS, well matched master curves were obtained, especially for the one case from THF/EAc (Figure 16a). This may be attributed to a more precise and easier determination of the yield point on the stress-strain plot due to its plastic-like nature. For the samples of SBS cast from CCl<sub>4</sub> and CH (Figures 16b and 17a), factors affecting the viscosity behaviour were not as complicated as those in multicomponent systems (Figures 16b and 17b). Therefore, the master curves for single component systems were better matched. In the dynamic test, the deformations of samples were <1% which was considerably smaller than those in the static test (>300%), and the degree of each factor contributing to the influences on viscosity was different for each test; therefore, a deviation between the curves of the dynamic and static tests was created. Another possible reason leading to this deviation was the effect of 'stress-hardening' observed by Pedemonte *et al.*<sup>24</sup>. They found that at large tensile deformation of SBS, the crystallinity of PBd segments increased as the extension ratio increased. The stress responding to this was greater than expected; therefore, it would create an increase in viscosity.

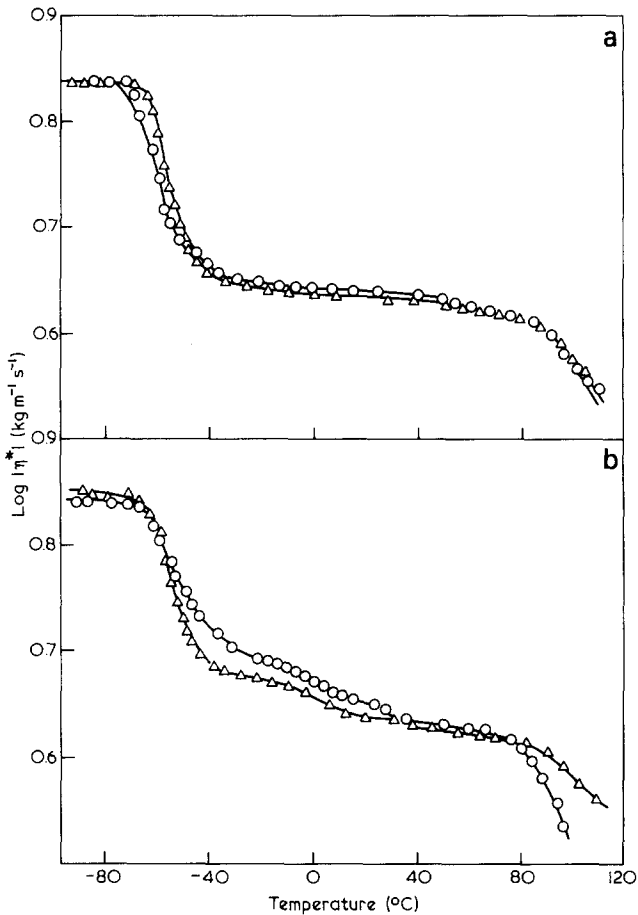


**Figure 9** Complex viscosity versus temperature. (a):  $\Delta$ , SBS from CCl<sub>4</sub>;  $\circ$ , SBS from CCl<sub>4</sub> annealed at 70°C for 12 h. (b):  $\Delta$ , SBS(70)+PS6(15)+PBd(15) from CCl<sub>4</sub>;  $\circ$ , SBS(70)+PS6(15)+PBd(15) from CCl<sub>4</sub> heated at 140°C for 45 min then quenched

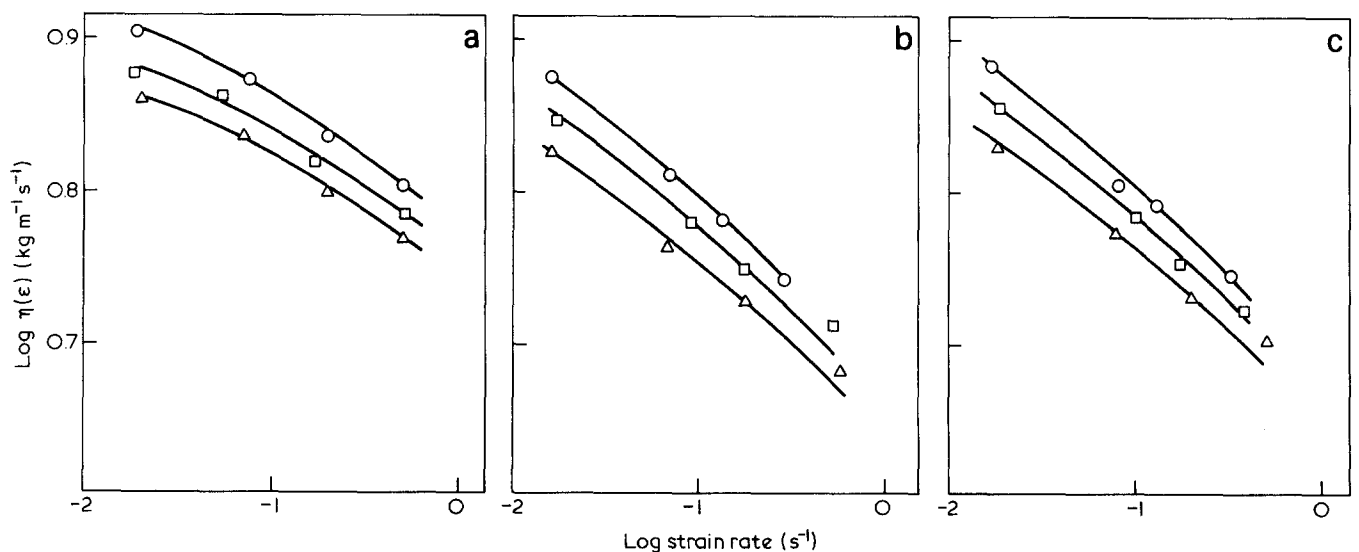


**Figure 10** Shear viscosity at different temperatures versus strain rate. (a) SBS from THF(50)/EAc(50); (b) SBS(80)+SBR(20) from CCl<sub>4</sub>; (c) SBS(70)+PS6(15)+PBd from CCl<sub>4</sub>.  $\circ$ , 35°C;  $\square$ , 65°C;  $\Delta$ , 80°C

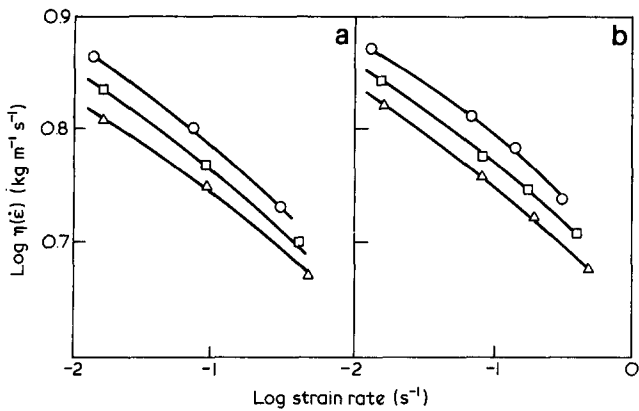


**Figure 11** Shear viscosity at different temperatures versus strain rate. (a) SBS from cyclohexane; (b) SBS from  $\text{CCl}_4$ .  $\circ$ , 35°C;  $\square$ , 65°C;  $\triangle$ , 80°C

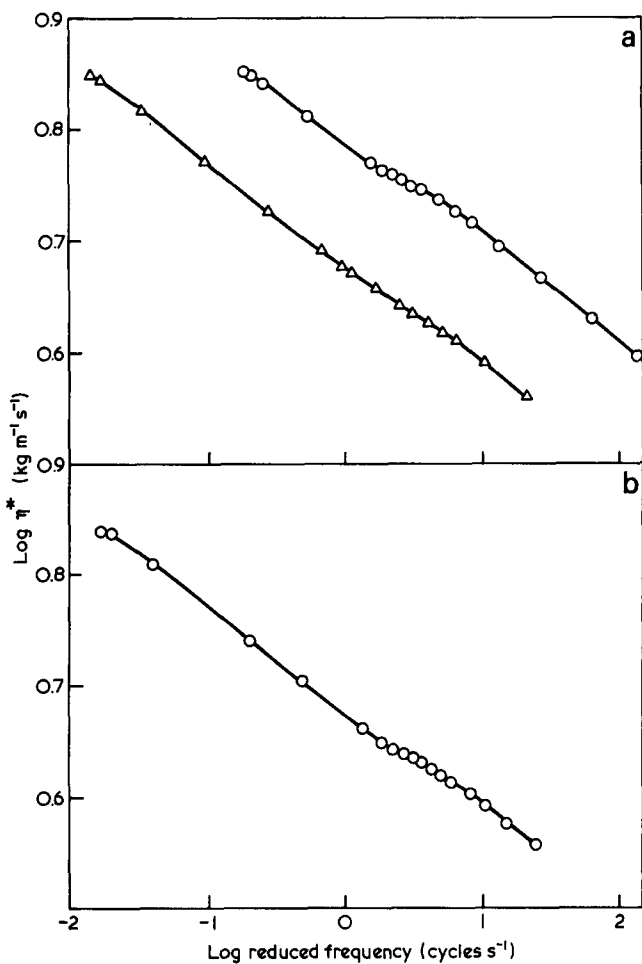


**Figure 12** Master curves from the dynamic experiments. Reference temperature, 35°C. (a):  $\circ$ , SBS from THF(50)/EAc(50);  $\triangle$ , SBS(70) + PS6(15) + PBd(15) from  $\text{CCl}_4$ . (b):  $\circ$ , SBS from  $\text{CCl}_4$

**CONCLUSIONS**

The results from the dynamic experiments show that the morphologies of SBS can be varied by using a different casting solvent. The solubility parameter of the casting solvent towards the individual block can affect the morphology thus formed. Swelling of the homopolymers added to the matrix and the domains results in a diffuse and thicker interphase between them. In addition, ther-

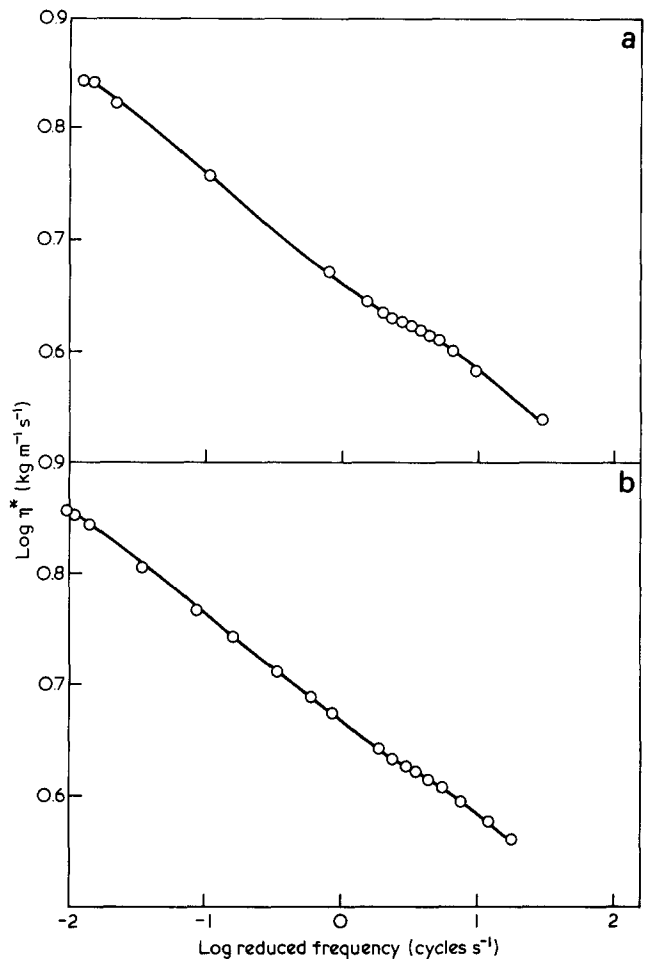


**Figure 13** Master curves from the dynamic experiments. Reference temperature, 35°C. (a):  $\circ$ , SBS from cyclohexane. (b): SBS(80) + SBR(20) from  $\text{CCl}_4$

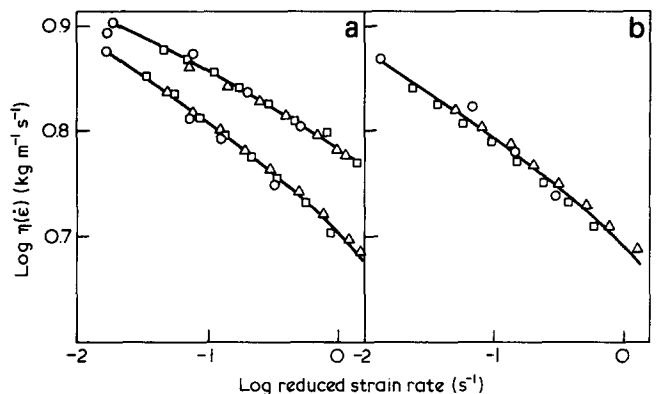


**Figure 14** Master curves from the static experiments. (a): A, SBS from THF(50)/EAc(50); B, SBS(70) + PS6(15) + PBd(15) from  $\text{CCl}_4$ . Reduced to 35°C. (b): SBS from  $\text{CCl}_4$ . Reduced to 35°C.  $\circ$ , 35°C;  $\square$ , 65°C;  $\triangle$ , 80°C

mal treatment can also lead to the same result. Therefore, the molecular relaxation mechanism between the two main transitions established by the authors is confirmed by the data. However, the inherent characteristics of the static experiment limit the amount of morphological detail that can be elucidated. Instead of using the WLF equation, the time-temperature superposition principle applied here also is shown to be successful.

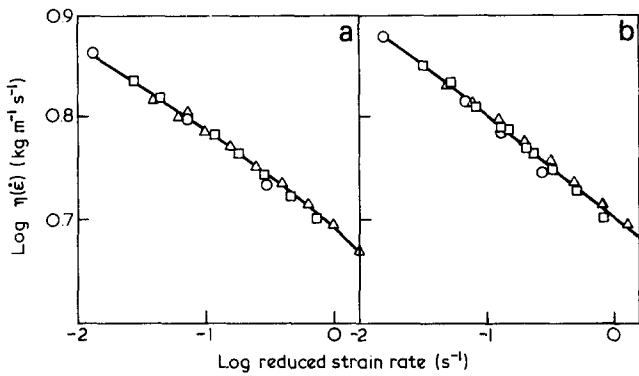


**Figure 15** Master curves from the static experiments. (a) SBS from cyclohexane. Reduced to 35°C. (b) SBS(80)+SBR(20) from CCl<sub>4</sub>. Reduced to 35°C. ○, 35°C; □, 65°C; △, 80°C

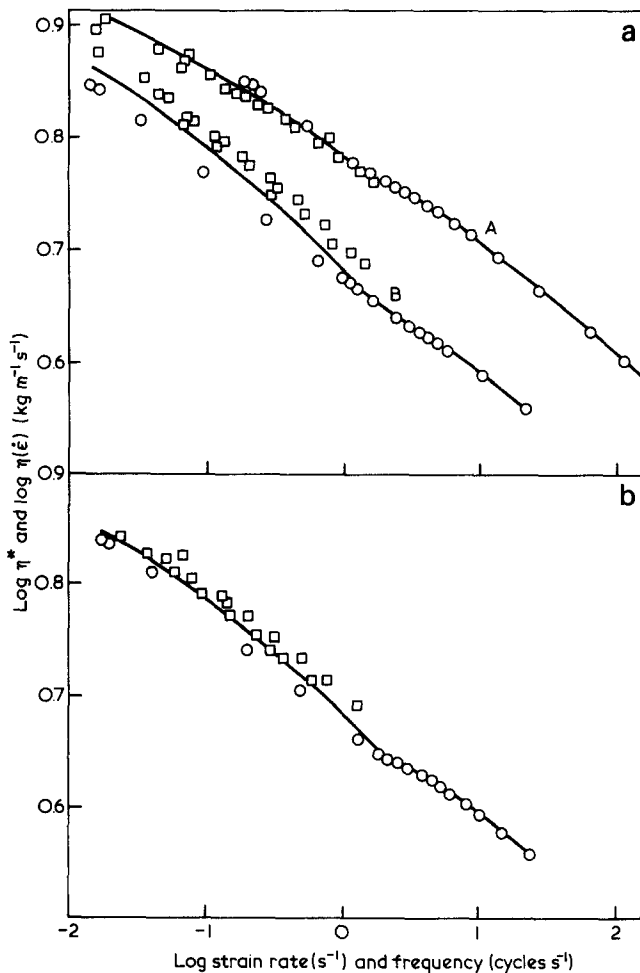


**Figure 16** Combined master curves from dynamic and static experiments. (a): A, SBS from THF(50)/EAc(50); B, SBS(70)+PS6(15)+PBd(15) from CCl<sub>4</sub>. (b) SBS from CCl<sub>4</sub>. ○, Dynamic data; □, stress-strain data

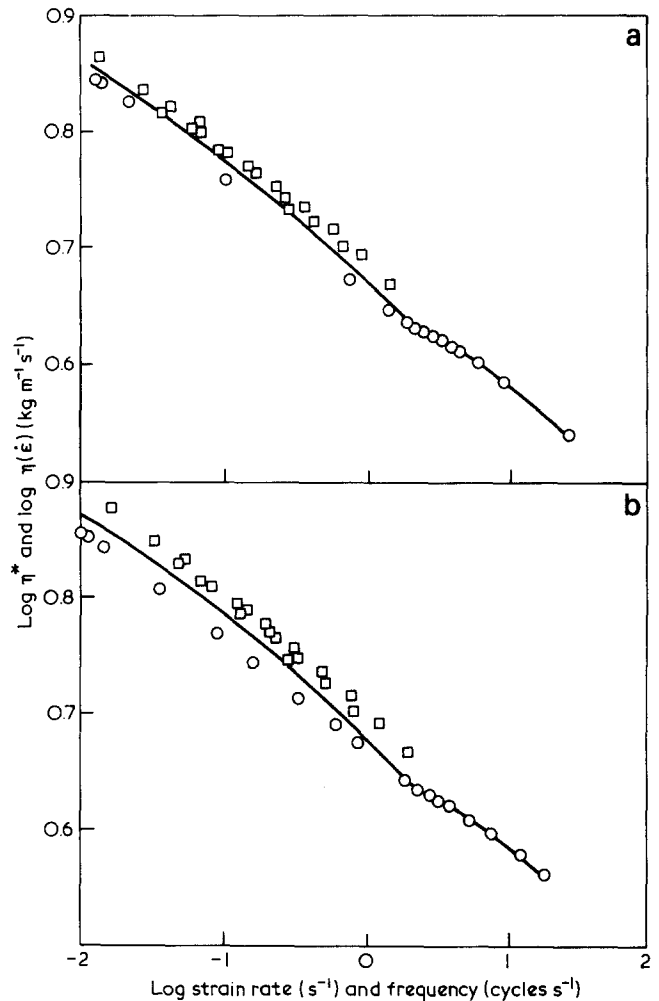


**Figure 17** Combined master curves from dynamic and static experiments. (a) SBS from cyclohexane. (b) SBS(80)+SBR(20) from CCl<sub>4</sub>. ○, Dynamic data; □, stress-strain data

REFERENCES

- 1 Holden, G., Bishop, E. T. and Legge, N. R. *J. Polym. Sci. (C)* 1969, **26**, 37
- 2 Inoue, T., Soen, T. T., Hashimoto, T. and Kawai, H. *J. Polym. Sci. (A-2)* 1969, **7**, 1283
- 3 Beecher, J. F., Marker, L., Bradford, R. D. and Aggarwal, S. L. *J. Polym. Sci. (C)* 1969, **26**, 117
- 4 Inoue, T., Moritani, M., Hashimoto, T. and Kawai, H. *Macromolecules* 1971, **4**, 500
- 5 McIntyre, D. and Campos-Lopez, E. in 'Block Copolymers' (Ed. S. L. Aggarwal), Plenum Press, New York, 1971, pp. 19-30

- 6 Pedemonte, E., Turturro, A., Bianchi, U. and Deretta, P. *Polymer* 1973, **14**, 145
- 7 Pedemonte, E., Dondero, G. and Alfonso, G. C. *Polymer* 1975, **16**, 531
- 8 Yeh, G. S. Y., Hosemann, R., Loboda Cackovic, J. and Cackovic, H. *Polymer* 1976, **17**, 309
- 9 Pedemonte, E., Dondero, G., Candia, F. and Romano, G. *Polymer* 1967, **17**, 72
- 10 Holden, G. in 'Block and Graft Copolymerization', (Ed. R. J. Ceresa), Wiley-Interscience, 1973, Vol. 1, Ch. 6
- 11 Chiang, N. T. and Sefton, M. V. *J. Polym. Sci. (Phys.)* 1977, **15**, 1927
- 12 Shen, M. and Kaelble, D. H. *J. Polym. Sci. (B)* 1970, **8**, 149
- 13 Morton, M. in 'Block Copolymers', (Ed. S. L. Aggarwal), Plenum Press, New York, 1970, pp. 1-17
- 14 Riess, V. G., Kohler, J., Journut, C. and Banderet, A. *Die Makromol. Chemie.* 1967, **101**, 58
- 15 Kraus, G. and Rollmann, K. W. *J. Polym. Sci. (Phys.)* 1976, **14**, 1133
- 16 Tung, L. H. *J. Appl. Polym. Sci.* 1979, **24**, 953
- 17 Runyon, J. R., Barnes, D. E., Rudd, J. F. and Tung, L. H., *Appl. Polym. Sci.* 1969, **13**, 2359
- 18 Nakajima, N. *Polym. Eng. Sci.* 1979, **19**, 215
- 19 Arnold, K. R. and Meier, D. J. *J. Appl. Polym. Sci.* 1970, **14**, 427
- 20 Szwarc, M., Levy, M. and Milkovich, R. *J. Am. Chem. Soc.* 1956, **78**, 2656
- 21 Brandup, J. and Immergut, E. H. 'Polymer Handbook', Interscience, New York, 1966
- 22 Beamish, A., Goldberg, R. A. and Hourston, D. J. *Polymer* 1977, **18**, 49
- 23 Meier, D. J. *Prepr., Am. Chem. Soc., Div. Polym. Chem.* 1973, **14**, 280; 1974, **15**, 171
- 24 Pedemonte, E., Alfonso, G. C., Dondero, G., Candia, F. and Araimo, L. *Polymer* 1977, **18**, 191